

# Vibrational Relaxation of Molecular Ions at Low Temperatures: $\text{O}_2^-(\nu=1) + \text{Ar}$

H. K. Shin

Department of Chemistry, University of Nevada, Reno, Nevada 89557

Received: January 5, 2005; In Final Form: March 31, 2005

The vibrational relaxation of oxygen molecular ions trapped in an argon cage in the temperature range 10–85 K has been studied using semiclassical procedures. The collision model is based on the trapped molecule undergoing the restricted motions (local translation and hindered rotation) in a cage formed by its 12 nearest argon neighbors in a face-centered cubic arrangement. At 85 K in the liquid argon temperature range, the relaxation rate constant of  $\text{O}_2^-(\nu=1)$  is  $1130 \text{ s}^{-1}$ . The rate constant decreases to  $270 \text{ s}^{-1}$  at 50 K and to  $3.90 \text{ s}^{-1}$  at 10 K in the solid argon temperature range. In the range 10–85 K, the rate constant closely follows the temperature dependence  $k \propto T^{2.7}$ . Energy transfer pathways for the trapped molecular ion are vibration to local translation, argon phonon modes, and rotation (both hindered and free).

## I. Introduction

Vibrational relaxation of molecular species trapped in a cluster environment is strongly dependent on the nature of host–guest interaction and the type of motion that the guest undergoes in the restricted space. When the interaction system is maintained at or near the cryogenic environment, the motion of the guest is severely limited to a narrow space in the cage surrounded by many solvent layers, providing an opportunity to study the time scales of energy transfer pathways associated with the restricted motion of the guest. When the guest is a diatomic molecule trapped in one full shell of a face-centered cubic (fcc) arrangement or an icosahedral arrangement of argon atoms,<sup>1–3</sup> the molecule finds enough space to translate in the cage, but a strong repulsive wall builds up when it moves away significantly from the center of the cage. The interaction of the molecule with host atoms in the repulsive region is responsible for causing perturbation of molecular vibration, thus leading to vibrational relaxation. For example, the spectroscopic data of HCN in the Ar, Kr, and Xe matrixes indicate that the molecule is trapped in a substitutional site of the fcc configuration at the cryogenic environment.<sup>4</sup> Such an Ar matrix environment has been used in theoretical studies of the addition dynamics of  $\text{F}_2$  to *cis*-ethylene- $d_2$  and the subsequent decomposition of the vibrationally excited 1,2-difluoroethane- $d_2$ .<sup>5</sup> Among other studies involving the fcc structure<sup>6–10</sup> is the calculation of the phonon thermal conductivity of the Lennard-Jones (LJ) argon crystal between 20 and 80 K using molecular dynamics simulations.<sup>11</sup> For the guest molecule confined to such a closely packed arrangement, the substitutional site is not large enough for the molecule to undergo free rotation and translation. Furthermore, the rotational motion is under the influence of a strong potential field, which leads the guest to experience a periodic or nearly periodic field as it rotates. Thus, both translational and rotational motions of the guest in the cage are hindered.<sup>3</sup> Molecular ions as large as  $\text{Br}_2^-$  and  $\text{I}_2^-$  are also known to be caged in an argon or  $\text{CO}_2$  environment, the systems that have been considered to study the microscopic nature of anion solvation and the effects of solvation on elementary chemical reactions.<sup>12–14</sup>

When the guest is charged, the induction energy can modify greatly the host–guest interaction, thus affecting the mechanisms of vibrational relaxation especially at low temperatures. The

induction energy deepens the attractive potential well over the neutral–neutral interaction and modifies the slope of the repulsive part of the interaction energy on which the efficiency of energy transfer depends sensitively.<sup>15</sup> Molecular ions have vibrational frequencies and bond distances different from their neutral counterparts. The frequency change leads to a change in the amount of energy to be transferred from the excited molecular ion, whereas the bond distance change alters the space available for the guest in the cage. Thus, these three factors, namely, the induction energy, vibrational frequency, and bond distance, are mainly responsible for molecular ions relaxing at a much different rate from uncharged molecules. Vibrational relaxation in condensed phases involves a number of energy transfer pathways and one of the major problems in the relaxation process is the time scale of energy transfer pathways to various motions.<sup>3,16–19</sup> For ionized guests, such a time scale can be significantly different from that of neutral molecules. The guest is in intimate contact with the host atoms, suffering at least  $10^{12}$  collisions per second. Despite such a high collision frequency, vibrational relaxation in condensed phases is known to be very slow compared to the gas-phase process,<sup>16</sup> indicating that these numerous collisions, each of which acts to perturb the vibrational motion, are highly ineffective in transferring energy. Another problem is the role of host in the relaxation, which is unique to the processes taking place in condensed media. Even in a one-shell environment, the vibrational motion of host atoms can contribute significantly to the relaxation process. In the condensed phase, therefore, there can be several important energy transfer pathways involving restricted translational and rotational motions as well as phonon modes, and the efficiency (or inefficiency) of each energy transfer pathway depends sensitively on the nature of interactions between the guest and host atoms, so the determination of time scales for energy transfer processes warrants detailed interpretation of all these motions involved.

In the condensed phase, time scales for vibrational relaxation for simple molecules are known to vary by many orders of magnitude. For example, the lifetime of vibrationally excited states  $\text{N}_2(\text{A } ^3\Sigma_u^+)$  in an argon matrix at 1.7–30 K is as long as 3 s,<sup>16,20</sup> and the lifetime of  $\text{O}_2(\text{X } ^3\Sigma_g^-)$  in liquid mixtures with Ar and  $\text{N}_2$  at 77 K is in the range of milliseconds,<sup>17,18</sup> whereas

the lifetime of heteronuclear species  $\text{NH}(\text{A } ^3\Pi)$  in Ar or  $\text{OH}(\text{OD}(\text{A } ^2\Sigma^+))$  in Ar is only about  $10^{-6}$  s in the temperature range 4.2–25 K.<sup>16,21</sup> Even in the latter systems, the time scale is much longer than the gas-phase values. Studies show that the relaxation rate constant of vibrationally excited oxygen molecules in argon is in the range of centi- to milliseconds.<sup>3,17–19</sup> Although vibration-to-rotation (VR) energy transfer is the principal pathway for the relaxation of hydrogenic heteronuclear diatomic molecules,<sup>22,23</sup> the pathway of vibration-to-translation (VT) energy transfer rather than the VR mechanism plays a leading role in relaxing vibrationally excited homonuclear diatomic molecules such as  $\text{O}_2$  and  $\text{N}_2$  in Ar.<sup>3,19</sup> When the guest is an ion, the attractive energy term introduced by the ion–atom interaction can significantly modify the translational motion, thus enhancing the perturbation of the vibrational motion. In a narrow cage space, the modified interaction energy can affect the influence of the potential field on rotation. Translation and rotation, both of which are confined to close proximity of the cage center, can now enhance vibrational relaxation over the neutral guest. Thus, these modified translations and rotations as well as the phonon modes of host atoms should be carefully considered in studying the vibrational relaxation of molecular ions in condensed media.

In the present paper, we study the relaxation of  $\text{O}_2^-(\nu=1)$  using an interaction model for the molecule that is trapped in a cage environment formed by 12 nearest argon neighbors, hence, a face-centered cubic arrangement. Our approach includes all atom–atom interactions for the guest and host atoms and uses the semiclassical perturbation theory, which relates the energy transfer probability to the Fourier integral of the time-dependent force.<sup>24</sup> The time dependence of the interaction energy is determined from the solution of the equation of motion for translation, which is localized in the neighborhood of the cage center. In addition to local translation, the motions responsible for sharing the energy released by the  $\text{O}_2^-(\nu=1)$  vibration are the rotation of the guest and the vibration of host atoms. Low-lying rotational states are considered to be hindered, whereas high-lying ones are free. We treat the vibrational and (hindered and free) rotational motions of  $\text{O}_2^-$  and the phonon modes of host atoms quantum mechanically in formulating energy transfer probabilities.

## II. Model

The interaction model for  $\text{O}_2$ –Ar has been reported in ref 3. We briefly recapitulate the essential aspects of the model and the effects resulting from inclusion of the induction energy. The positions of 12 Ar atoms in a fcc arrangement are shown in Figure 1a. The configuration corresponds to the atoms occupying the midpoints of the 12 edges of a cube. Each atom of the guest molecular ion ( $\text{O}_A$  or  $\text{O}_B$ ) encounters the repulsive field created by the host atoms when  $\text{O}_2^-$  moves around in the cage. The two atoms undergo a series of collisions with the host atoms as the vibrationally excited guest translates and rotates. Each atom of  $\text{O}_2^-$  interacts with the 12 Ar atoms. These  $\text{O}_{A(B)}$ –Ar interactions are represented by the LJ (12–6) potential. The Ar–Ar interaction energies are also represented by the LJ potential. The overall interaction potential energy is then the sum of these atom–atom interactions and the induction energy. In the region of strong repulsive interaction, the vibrational motion couples with local translation and rotation as well as the motion of host atoms; thus all these motions participate in the vibrational relaxation of  $\text{O}_2^-$  as energy accepting modes. The vibrational relaxation process is viewed as energy flow from the high-frequency mode to local translation, rotation (both

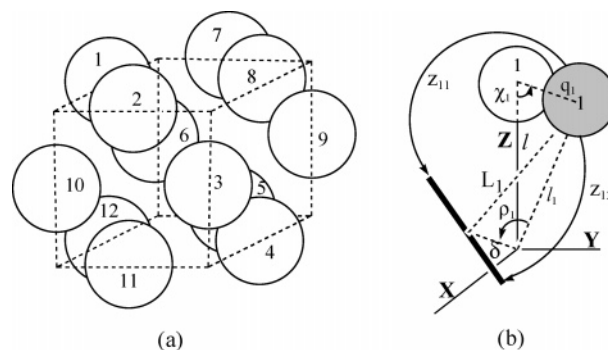


**Figure 1.** (a) Face-centered cubic structure, where 12 nearest neighbors occupy the midpoints of the 12 edges of a cube. Argon atoms 1, 2, ..., 6 are in one plane; 7, 8, and 9 are above that plane; 10, 11, and 12 are below. (b) Displacement of the c.m. of  $\text{O}_2^-$  from the cage center is  $\delta$  and that of argon atom 1 from its equilibrium position is  $q_1$ . The displaced atom is expressed by a filled circle. The argon 1 to c.m. of  $\text{O}_2^-$  distance is  $L_1$  and that to cage center distance is  $l_1$ . Also shown are the Ar–O distances  $z_{11}$  and  $z_{12}$ .

hindered and free) by multirotational quantum processes, and the phonon modes of host atoms.

We choose Ar atom 1 to be in the Z-axis so that  $\theta$  measures the rotation of the molecular axis from this axis and  $\phi$  is the azimuth on the XY plane. The coordinates needed to derive the interaction energy are shown in Figure 1b. The displacement  $\delta$  can be expressed in terms of  $L_1$ ,  $l_1$ , and  $\rho_1$ . The instantaneous bond distance of  $\text{O}_2^-$  is  $d + x$ , where  $x$  is the displacement of the bond distance from its equilibrium value  $d$ . Thus, we introduce the spherical coordinate system  $(x, \theta, \phi)$  into 24 O–Ar distances to set up the overall interaction energy. In determining the size of the cage space available for the motion of  $\text{O}_2^-$ , we note the crystal radius of 1.92 Å for Ar,<sup>25</sup> so the Ar–Ar distance or the distance between Ar and the center of cage is  $l = 3.84$  Å. Because the bond distance of  $\text{O}_2^-$  and orbital radius of O are 1.35 Å<sup>26</sup> and 0.45 Å,<sup>25</sup> respectively, the argon and oxygen orbitals are separated by at least 0.80 Å when the center of mass (c.m.) of  $\text{O}_2^-$  is at the cage center. When  $\text{O}_2^-$  translates close to argon atoms, it encounters a sharply rising repulsive wall, where the perturbation of the vibrational motion occurs.

## III. Interaction Energies

The interaction model for  $\text{O}_2 + \text{Ar}$  has been reported in ref 3 and the same procedure will be adopted here whenever applicable. Both atoms of the guest molecular ion interact with all host atoms. Including all these 24 O–Ar interactions, the induction energy and the argon–argon interaction terms, we can express the overall interaction energy in the form

$$U(L_n, x, \theta, \phi) = \sum_{n=1}^{12} \sum_{i=1}^2 V_{ni}[z_{ni}(L_n, x, \theta, \phi)] + \sum_{n=1}^{12} V_{\text{ind}}(L_n) + \sum_{k \neq l} V_{\text{Ar}}(z_{kl}) \quad (1)$$

where  $L_n$  is the distance between the  $n$ th Ar and the c.m. of  $\text{O}_2^-$ , which will determine the value of  $\delta$  for local translation ( $L_1$  is shown in Figure 1b), and  $z_{kl}$  is the distance between argon  $k$  and  $l$ . The second sum is for the interaction between the charge of  $\text{O}_2^-$  and the dipole moment induced in Ar. For the  $n$ th argon atom, when two Ar–O distances are distinguished by the indices  $n_1$  and  $n_2$  (i.e.,  $i = 1$  and  $2$ ) in the first term, the distances between the O atoms and 12 Ar atoms are

$$z_{n_1}, z_{n_2} = [L_n^2 + 1/4(d+x)^2 \mp L_n(d+x)f_n(\theta, \phi)]^{1/2} \quad (2)$$

where the angle factors determining the orientation of the molecular axis with respect to the host atoms are

$$f_n(\theta, \phi) = \cos[(n-1)\pi/3]\cos\theta + \sin[(n-1)\pi/3]\sin\theta\cos\phi \text{ for } n = 1-6$$

$$f_7(\theta, \phi) = -3^{-1/2}[2^{1/2}\sin\phi - \cos(\pi/6)\cos\theta - \cos(\pi/6)\sin\theta\cos\phi]$$

$$f_8(\theta, \phi) = -3^{-1/2}[2^{1/2}\sin\phi - \cos(5\pi/6)\cos\theta - \cos(5\pi/6)\sin\theta\cos\phi]$$

$$f_9(\theta, \phi) = -3^{-1/2}[2^{1/2}\sin\phi - \cos(9\pi/6)\cos\theta - \cos(9\pi/6)\sin\theta\cos\phi]$$

$$f_{10}(\theta, \phi) = -3^{-1/2}[2^{1/2}\sin\phi + \cos(3\pi/6)\cos\theta + \cos(3\pi/6)\sin\theta\cos\phi]$$

$$f_{11}(\theta, \phi) = -3^{-1/2}[2^{1/2}\sin\phi + \cos(7\pi/6)\cos\theta + \cos(7\pi/6)\sin\theta\cos\phi]$$

$$f_{12}(\theta, \phi) = -3^{-1/2}[2^{1/2}\sin\phi + \cos(11\pi/6)\cos\theta + \cos(11\pi/6)\sin\theta\cos\phi]$$

To describe the many-body dynamics in the present model, we first note that the c.m. of  $O_2^-$  moves around the center of the cage by  $\delta$ , as shown in Figure 1b. When the c.m. is positioned at the cage center, the values of all  $L_n$  are equal to each other and coincide with  $l$ . In terms of the coordinates defined in Figure 1b, we can express the distance between the  $n$ th Ar atom and the c.m. of  $O_2^-$  as  $L_n = [l_n^2 + \delta^2 - 2l_n\delta\cos\rho_n]^{1/2}$ , where  $l_n = [l^2 + q_n^2 - 2lq_n\cos\chi_n]^{1/2}$  and  $\rho_1$  is shown in Figure 1b. The angle  $\chi_n$  measures the direction of the displacement  $q_n$  from the axis of the cage center to  $n$ th argon. Thus, we have two other sets of angles ( $\rho_n$  and  $\chi_n$  and their azimuths) in addition to the molecular rotation angles ( $\theta, \phi$ ), but these sets describing the position of the c.m. of  $O_2^-$  and the displacement of Ar from its equilibrium position have no effect on the molecular rotation, so they do not contribute to the relaxation process. Therefore, the effects of these two sets can be replaced by their orientation-averaged values.

When we use the LJ (12-6) potential, the overall interaction energy becomes

$$U(L_n, x, \theta, \phi) = 2\epsilon \sum_{n=1}^{12} \sum_{i=1}^2 \left[ \left( \frac{\sigma}{z_{ni}} \right)^{12} - \left( \frac{\sigma}{z_{ni}} \right)^6 \right] + \sum_{n=1}^{12} \frac{1}{4\pi\epsilon_0} \frac{e^2\alpha}{2L_n^4} + 4\epsilon_{Ar} \sum_{k \neq l} \left[ \left( \frac{\sigma_{Ar}}{z_{kl}} \right)^{12} - \left( \frac{\sigma_{Ar}}{z_{kl}} \right)^6 \right] \quad (3)$$

where the interaction and spectroscopic constants are  $\omega_e = \omega/2\pi = 1090 \text{ cm}^{-1}$ ,  $\omega_{ex_e} = 8.1 \text{ cm}^{-1}$ , bond distance  $d = 1.35 \text{ \AA}$ ,<sup>26</sup> and  $\epsilon/k = 118.6 \text{ K}$ .<sup>27</sup> In the induction energy,  $\epsilon_0$  is the vacuum permittivity,  $\alpha$  is the polarizability of Ar, which is  $1.64 \text{ \AA}^3$ ,<sup>28</sup> and  $e$  is the electronic charge. Because the induction energy is independent of the molecular bond displacement and orientation, it does not contribute to the perturbation energy, which is responsible for vibrational and rotational transitions. However, the induction energy introduces a significant attractive energy in the overall interaction energy, thus creating a deeper attractive well for the molecule to “speed up” toward the host atoms; i.e., it modifies the collision trajectory to increase the efficiency of

energy transfer. The equilibrium distance between  $O_2^-$  and the host atom is  $2^{1/6}\sigma = 3.92 \text{ \AA}$ , where  $\sigma = 3.49 \text{ \AA}$ .<sup>27</sup> The values of  $\sigma$  and  $\epsilon$  for  $O_2^- + \text{Ar}$  needed in determining the first term of eq 3, are obtained from  $\epsilon_{Ar}/k = 119.8 \text{ K}$ ,  $\epsilon_{O_2^-}/k = 117.5 \text{ K}$ ,  $\sigma_{Ar} = 3.405 \text{ \AA}$ , and  $\sigma_{O_2^-} = 3.58 \text{ \AA}$  using the usual combination rules for mixtures.<sup>27</sup> Note that the equilibrium distance between  $O_2^-$  and Ar is significantly shortened from the  $O_2^- + \text{Ar}$  value given above because of the contribution of the induction energy.

The function  $U(L_n, x, \theta, \phi)$  depends on the pertinent coordinates in a complicated manner, but we can recast it in a form that shows the coupling of the molecular vibration with the rest of the coordinate system in an explicit form for the present study, which employs semiclassical perturbation procedures. The Ar–Ar interaction energy in eq 3 is not directly coupled to the internal motions of the molecule, but its atom–atom distance depends on the displacement  $q_n$ , determining the frequency and in turn the amount of energy transfer from  $O_2^-$  to the phonon modes. Equation 3 can now be written in the Taylor expansion for a function of three variables as

$$U = U(L_n, x, \theta, \phi)|_{x=0, \{q\}=0, \delta=0} + \sum_{s=1}^{\infty} (1/s!) \left( x \frac{\partial}{\partial x} + \delta \frac{\partial}{\partial \delta} + q_n \frac{\partial}{\partial q_n} \right)^s U(L_n, x, \theta, \phi)|_{x=0, \{q\}=0, \delta=0} \quad (4)$$

where  $\{q\}$  is a collective notation for  $q_1, q_2, \dots, q_{12}$ , the derivatives are evaluated at  $x = 0$ ,  $\delta = 0$ , and  $\{q\} = 0$ , and  $L_n$  is dependent on  $\delta$  and  $q_n$ . The operation produces the terms containing  $\cos^2\rho_n$ , which is  $1/3$  when averaged over the solid angles. In averaging  $\cos\chi_n$ , we note that each Ar atom on the cage directs its interaction to  $O_2^-$ , so its inward motion ranges from 0 to  $\pi$  and its azimuthal from 0 to  $2\pi$ . The average of  $\cos\chi_n$  in this inward angle range is  $1/2$ . Though the one-quantum transition of  $O_2^-$  requires the presence of the coordinate  $x$  for  $1 \rightarrow 0$  and the phonon mode  $q_n$  for phonon transitions  $k \rightarrow k+1$ , the displacement of local translation is quadratic in  $\delta$ , so after straightforward differential operations, we arrive at the perturbation energy term

$$\frac{15}{4!} \frac{\partial}{\partial x} \frac{\partial}{\partial q_n} \frac{\partial^2}{\partial \delta^2} U(L_n, x, \theta, \phi)|_{x=0, \delta=0, \{q\}=0} \delta^2 q_n x = 2\epsilon \sum_{n=1}^{12} \sum_{i=1}^2 \left\{ \left[ 252 \left( \frac{\sigma}{l} \right)^{12} G_{ni}^{-10} - 30 \left( \frac{\sigma}{l} \right)^6 G_{ni}^{-7} \right] \left( \frac{d}{2l} \mp f_n \right) \times \left( -2 \mp \frac{d}{l} f_n \right)^3 + \left[ 84 \left( \frac{\sigma}{l} \right)^{12} G_{ni}^{-9} - 30 \left( \frac{\sigma}{l} \right)^6 G_{ni}^{-6} \right] \left( 2 \mp \frac{d}{l} f_n \right) \times \left[ \left( \frac{d}{l} f_n^2 \mp 2f_n \right) + \left( \frac{10}{3} \mp \frac{4d}{3l} \right) \left( \frac{d}{2l} \mp f_n \right) \right] + \left[ \frac{21}{2} \left( \frac{\sigma}{l} \right)^{12} G_{ni}^{-8} - 3 \left( \frac{\sigma}{l} \right)^6 G_{ni}^{-5} \right] \left[ \pm \frac{2}{3} \left( 10 - \frac{d^2}{l^2} f_n - \frac{4d}{l} f_n^2 \right) \pm \left[ \frac{3}{2} \left( \frac{\sigma}{l} \right)^{12} G_{ni}^{-7} - \frac{3}{4} \left( \frac{\sigma}{l} \right)^6 G_{ni}^{-4} \right] \frac{4}{3} f_n \right] \left( \frac{\delta}{l} \right)^2 \left( \frac{q_n}{l} \right) \left( \frac{x}{l} \right) \right\} \equiv 2\epsilon \sum_{n=1}^{12} \sum_{i=1}^2 U'(\theta, \phi) \left( \frac{\delta}{l} \right)^2 \left( \frac{q_n}{l} \right) \left( \frac{x}{l} \right) \quad (5)$$

where  $G_{ni} = [1 \mp (d/l)f_n(\theta, \phi) + (d/2l)^2]$  with  $i = 1$  for the upper sign and  $i = 2$  for the lower and  $f_n = f_n(\theta, \phi)$  for brevity.

#### IV. Transition Probabilities

The probability of energy transfer from  $O_2^-(\nu=1)$  to local translation, rotation, and phonon modes can be determined from the solution of the time-dependent Schrödinger equation<sup>23,24,29</sup>

$$i\hbar \frac{\partial \Psi}{\partial t} = [H_0 + U'(\delta, \{q\}, x, \theta, \phi)] \Psi \quad (6)$$

where  $H_0 = H_0^{\text{vib}} + H_0^{\text{rot}} + H_0^{\text{Ar}}$ , the Hamiltonian of the unperturbed system. The time evolution of the interaction system is described by the trajectory of local translation  $\delta(t)$ , which is the solution of the equation of motion for the guest molecule in the cage written as  $t = (\mu/2)^{1/2} \int_{\delta_0}^{\delta} [E - U(\delta)]^{-1/2} d\delta$ , where  $\mu$  is the reduced mass of the  $O_2^-$ -Ar system and  $E$  is the translational energy in the cage. To determine the trajectory  $\delta(t)$ , we need the  $\delta$ -dependent energy  $U(\delta)$ , which includes the contribution of the induction energy. When eq 2 is substituted in eq 3, the leading term of each interaction is  $L_n^{-12}$  and  $L_n^{-6}$ , which can be expanded in a power series of  $(\delta/l)$ , which converges rapidly because  $l = 3.84 \text{ \AA}$  and  $(\delta/l) \ll 1$ . The resulting expression is a function of  $\delta$  and  $\rho_n$ . When the  $\rho_n$  dependence is averaged over the solid angles as mentioned above following eq 4, the result appears in the quadratic form  $U(\delta) = V_0(\delta/l)^2$ , where  $V_0$  is an energy constant containing the inverse-power terms in  $l$ ,  $V_0 = 12[22(\sigma/l)^{12} - 5(\sigma/l)^6 - (1/4\pi\epsilon_0)(e^2\alpha/2l^4)]$ . The lower integration limit is then  $\delta_0 = l(E/V_0)^{1/2}$ , so the integration of the equation of motion yields the oscillatory function

$$\delta(t) = l(E/V_0)^{1/2} \cos[(2V_0/\mu)^{1/2}(t/l)] \quad (7)$$

The local translational motion in a free volume of the cage is then a periodic function of time with the period  $\tau = \pi l(2\mu/V_0)^{1/2}$ .

The general solution of eq 6 appears in the standard form

$$\Psi(x, \theta, \phi) = \sum_{vjm} C_{vjm}(t) \psi_v(x) Y_{jm}(\theta, \phi) \xi_k(q_n) \exp[-(i/\hbar)(E_v^{\text{vib}} + E_j^{\text{rot}} + E_k^{\text{Ar}})t] \quad (8)$$

where  $\psi_v(x)$  is the vibrational wave function and  $Y_{jm}(\theta, \phi)$  is the spherical harmonics, the energies satisfying the eigenvalue equations  $H_0^{\text{vib}}\psi_v(x) = E_v^{\text{vib}}\psi_v(x)$ ,  $H_0^{\text{rot}}Y_{jm}(\theta, \phi) = E_j^{\text{rot}}Y_{jm}(\theta, \phi)$  and  $H_0^{\text{Ar}}\xi_k(q_n) = E_k^{\text{Ar}}\xi_k(q_n)$ . The expansion coefficients  $C_{vjm}(t)$  provide a complete description of the dynamics throughout the interaction, and they can be explicitly determined by substituting eq 8 in eq 6:

$$C_{v'j'm'k', vjm}(t) = -(i/\hbar) \left( \frac{5\epsilon}{8l^2} \right) \left( \frac{E}{V_0} \right) \langle v'|x|v \rangle \langle k'|q_n|k \rangle \times \left\langle j'm' \left| \sum_{n=1}^{12} \sum_{i=1}^2 U'(\theta, \phi) \int_{-l}^l \cos^2 \left[ (2V_0/\mu)^{1/2} \frac{t'}{l} \right] e^{i\Delta E_{j',k',k}/\hbar} dt' \right| jm \right\rangle \quad (9)$$

where  $\Delta E_{j',k',k}$  is the amount of energy transfer from vibration to local translation (see below). The vibrational matrix element for  $1 \rightarrow 0$  is  $\langle 0|x|1 \rangle = (\hbar/2M\omega)^{1/2}$ , where  $M$  is the reduced mass of  $O_2^-$ . Assuming the harmonic oscillation, we obtain  $\langle k'|q_n|k \rangle = (k+1)^{1/2}(\hbar/2M_{\text{Ar}}\omega_{\text{Ar}})^{1/2}$  for  $k' = k+1$ , where  $M_{\text{Ar}}$  is the mass of Ar and  $\omega_{\text{Ar}}$  is the frequency of the phonon mode. The relaxation leads to  $O_2^-(\nu=1)$  releasing energy  $E_1 - E_0 = \hbar\omega$ , whereas rotation shares  $(E_j - E_i)$  and argon's phonon modes take  $(E_{k'} - E_k)$ , so the amount of energy transferred to local translation is  $\Delta E_{j',k',k} = \hbar\omega - (E_j - E_i) - (E_{k'} - E_k)$ . To

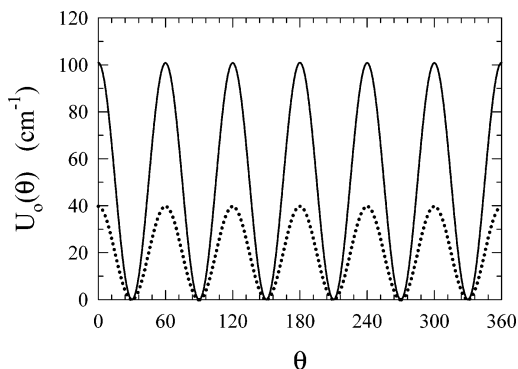


**Figure 2.** Dependence of the interaction energy on  $\theta$  for eq 3 with  $\phi = 0$  and  $L_n = l$ . The  $\nu_h = 0$  and 1 levels of the librational motion are indicated. The dotted curve for  $O_2 + \text{Ar}$  is shown for comparison.

evaluate the Fourier integral in eq 9, we note that the c.m. of  $O_2^-$  undergoes a one-half period oscillation out of the cage center during which the two oxygen atoms interact with the host atoms: i.e., the oxygen atoms sample the entire interaction field produced by the host atoms. This period corresponds to the interval from the lower limit  $-1/4\tau$  to the upper limit  $+1/4\tau$ , for which the integral can be readily evaluated.

In treating the role of rotational motion in the relaxation process, we note an important situation: motion is hindered, especially in low-lying energy levels. When there is a barrier to rotation, motions corresponding to low-lying energy levels may become hindered and transform into libration. The height of such a barrier is dependent on the strength of interaction between the guest molecule and host atoms. At low temperatures considered in the present study, only such low-lying levels are significantly populated, so the initial state of rotational motion can be dominated by libration; i.e., rotational transitions transform into hindered  $\rightarrow$  hindered and hindered  $\rightarrow$  free, as well as free  $\rightarrow$  free for sufficiently high-lying levels. In Figure 2, we plot the first part of eq 4 as a function of  $\theta$  for  $\phi = 0$ . The plot shows the barrier height of  $\Delta E^{\text{rot}} = 101 \text{ cm}^{-1}$ , which changes negligibly when  $\phi$  is varied. For example, for  $\phi = 0^\circ$ ,  $45^\circ$ , and  $90^\circ$ ,  $\Delta E^{\text{rot}} = 100.80$ ,  $100.80$ , and  $100.77 \text{ cm}^{-1}$ , respectively, where we show five significant figures for comparison. That is, hindered rotation is essentially independent of  $\phi$ . Thus we refer the part to as  $U_0(\theta)$ . If the barrier to rotation is higher than the rotational energy, then the rotation is hindered and the guest molecule librates about the minima of  $U_0(\theta)$ , which occur at  $\pi/6$ ,  $3\pi/6$ , ...,  $11\pi/6$ , satisfying the 6-fold symmetry. Also shown in Figure 2 for comparison is the curve for the  $O_2 + \text{Ar}$  case, where the barrier height is only  $39.8 \text{ cm}^{-1}$ .<sup>3</sup> The difference in these two systems is not from the induction energy, which is independent of  $\theta$ , rather from 24 atom-atom interaction energy terms that are dependent on the bond distance as shown in eq 2. It is important to note that the curve fits perfectly to the potential function  $U(\theta) = 1/2\Delta E^{\text{rot}}[1 + \cos(6\theta)]$ . The first eight rotational levels are hindered, i.e.,  $E_j^{\text{rot}} < \Delta E^{\text{rot}}$ , and the emerging motion is libration in the  $\nu_h = 0$  and 1 states. To the harmonic oscillator approximation we then find the frequency of the hindered motion to be  $\omega_{\text{lib}} = 6(\Delta E^{\text{rot}}/2I)^{1/2}$ ,<sup>30</sup> giving  $64.8 \text{ cm}^{-1}$  or the lowest level of the hindered motion ( $\nu_h = 0$ ) being  $32.4 \text{ cm}^{-1}$ . Here  $I$  is the moment of inertia of  $O_2^-$ . On the other hand, if  $\Delta E^{\text{rot}} < E_j^{\text{rot}}$ , then the rotation is free and the transition from the librational level  $\nu_h = 0$  or 1 to such a high-lying free rotational level is a hindered-to-free process. Thus, the rotational motion of  $O_2^-$  in the cage at and near cryogenic environments now leads to hindered-to-hindered, hindered-to-free, and free-to-free transitions. These

transitions will accompany vibration-to-local translation and vibration-to-argon's phonon mode energy transfer processes.

By use of the linear variational method, we obtain the wave functions for the lowest and first excited states of the hindered motion as

$$\Phi_{\nu_h}(\theta) = N_{\nu_h} \sum_{i=1}^6 \Xi_{\nu_h i}(\theta) \quad (10)$$

where  $\Xi_{0i}(\theta) = (\alpha/\pi)^{1/4} \exp[-1/2\alpha(\theta - i\pi/6)^2]$ ,  $\Xi_{1i}(\theta) = (\alpha/\pi)^{1/4}(2\alpha)^{1/2}(\theta - i\pi/6) \exp[-1/2\alpha(\theta - i\pi/6)^2]$ ,  $\alpha = [U''(\theta)|_{\theta=0}]^{1/2}/\hbar$ , and the normalization constants  $N_{\nu_h} = \{\int_{-\infty}^{+\infty} \Xi_{\nu_h i}(\theta)^2 d\theta\}^{-1/2}$  are 0.4081 and 0.4105 for  $\nu_h = 0$  and 1, respectively.

From eq 9, the probability of transition from  $|vjmk\rangle$  to  $|v'j'm'k\rangle$  with  $\Delta E_{j'k'k}$  transferred to local translation in the limit  $t \rightarrow \infty$  is then

$$P_{0j'm'k,1jmk}(E) = |C_{0j'm'k,1jmk}(\infty)|^2 \quad (11)$$

where we set  $\nu = 1$  and  $\nu' = 0$  for the relaxation process. To derive the energy transfer probability and in turn the relaxation rate constant, we have to average eq 11 over the thermal distribution of  $E$  and sum the resulting expression over the rotational states of  $O_2^-$  and the phonon states of host atoms. From eq 9, we note that the probability  $P_{0j'm',1jmk}(E)$  is proportional to  $E^2$ . Because the molecule confined in the cage travels at low velocities, we carry out the  $E$ -integration from zero to the average translation energy  $E^* = 3/2kT$  for the molecule translating in the three-dimensional cage. In treating free-to-free or free-to-hindered transitions, we note that the role of initial relative angular momentum can be replaced by its classical analogue, the impact parameter  $b$ . A reasonable approach to introduce the impact parameter in such transitions is to replace  $E$  by  $E(1 - b^2/l^2)$ , the modification which is known as the method of modified wavenumber, first introduced by Takayanagi<sup>31</sup> in the calculation of rotational transition probabilities.<sup>32</sup> This approach leads to  $P_{0j'm'k,1jmk}(E,b)$ , which then has to be averaged over  $b$  as  $2\pi \int_0^{b^*} P_{0j'm'k,1jmk}(E,b) b db / (\pi l^2)$  along with the thermal average. The upper limit of the integration range represents the maximum distance the c.m. of  $O_2^-$  can travel in the cage, which is  $\delta_{\max} = l(E/V_0)^{1/2}$  from eq 7. With these averaging and summing procedures, we now obtain the temperature-dependent deexcitation probability in the lengthy, but straightforward, expression<sup>3</sup>

$$P_{01}(T) = \frac{2\pi}{\pi(lkT)^2 Q_{Ar}(T) Q_{rot}(T)} \sum_{k,k'} e^{-E_k/kT} \sum_{j,j'} e^{-E_j^{rot}/kT} \sum_{m'=-j}^{+j} \sum_{m=-j}^{+j} \times \int_0^{b^*} \int_0^{E^*} P_{0j'm'k,1jmk}(E,b) e^{-E/kT} E dE b db \quad (12)$$

where  $Q_{rot}(T)$  is the rotational partition function. For the argon state sum, we have the thermal average  $Q_{Ar}^{-1} \sum_{k,k'} e^{-E_k/kT}$ , where the  $k,k'$ -sum operates on  $|k'q_n|k\rangle^2$  as well as  $\Delta E_{j'k'k}$  in  $P_{0j'm'k,1jmk}(E,b)$  in addition to  $e^{-E_k/kT}$ , thus leading to  $Q_{Ar}^{-1} \sum_{k,k'} (k+1) e^{-(k+1/2)\hbar\omega_{Ar}/kT}$  for  $k \rightarrow k'$ , where  $Q_{Ar}$  is the partition function for Ar oscillating with  $\omega_{Ar}$  about its equilibrium position. We obtain  $\omega_{Ar} = 2.16 \times 10^{12} \text{ s}^{-1}$  or  $11.5 \text{ cm}^{-1}$  from the force constant, i.e., the second derivative of eq 3 with respect to the displacement  $q_n$ , and the matrix element for single-phonon processes  $\langle k+1|q_n|k\rangle = 1.92 \times 10^{-9} (k+1)^{1/2} \text{ cm}$ . The  $E,b$ -integrated quantity in eq 12 can then be expressed as  $P_{0j'm'k,1jmk}$

( $T$ ), the sum of which over  $j'jm'k'k$  is the overall energy transfer probability  $P_{01}(T)$ .

## V. Results and Discussion

**A. Energy Transfer Probabilities.** Several energy transfer pathways operate in the relaxation of  $O_2^-$ . They are energy transfer from the excited molecular ion to local translation, phonon modes, and rotation. As noted above, low-lying rotational states are hindered, thus transforming rotational transitions to hindered-to-hindered and hindered-to-free, as well as free-to-free transitions. The energy transfer probability  $P_{01}(T)$  given by eq 12 is expressed for the rotation undergoing free-to-free transitions, which are associated with the matrix element

$$\langle j'm' | \sum_{n=1}^{12} \sum_{i=1}^2 U'(\theta, \phi) | jm \rangle = \int_0^{2\pi} \int_0^\pi Y_{j'm'}(\theta, \phi) \sum_{n=1}^{12} \sum_{i=1}^2 U'(\theta, \phi) Y_{jm}(\theta, \phi) \sin \theta d\theta d\phi \quad (13)$$

In this pathway, the amount of energy transfer to rotation is  $(E_j' - E_i)$ , to phonon modes is  $(E_s' - E_s)$ , and the rest of the vibrational energy,  $\Delta E_{j'k'k}$ , deposits in local translation.

For  $j = 0-8$ ,  $E_j^{rot} < \Delta E^{rot}$  and the rotational states have transformed into the vibrational state  $\nu_h = 0$  and 1, so the energy transfer pathway hindered-to-hindered transitions (namely,  $0 \rightarrow 0$ ,  $0 \rightarrow 1$ ,  $1 \rightarrow 1$ ) with the inelasticity  $\Delta E_{\nu_h' \nu_h k' k} = \hbar\omega - (E_{\nu_h'} - E_{\nu_h}) - (E_{k'} - E_k)$ , where  $\nu_h$  and  $\nu_h'$  now replace the rotational quantum numbers  $j, j'$ . In this case, the energy released by relaxing  $O_2^-(\nu=1)$  is transferred to local translation, phonon modes, and libration, so the rotational matrix element given above should be replaced by

$$\langle \nu_h' | \sum_{n=1}^{12} \sum_{i=1}^2 U'(\theta, \phi) | \nu_h \rangle = \int_{-\infty}^{+\infty} \Phi_{\nu_h'}(\theta) \sum_{n=1}^{12} \sum_{i=1}^2 U'(\theta, \phi) \Phi_{\nu_h}(\theta) d\theta \quad (14)$$

Because the value of the integrand with  $\Phi_{\nu_h}(\theta)$  given by eq 10 decreases rapidly as  $\theta$  moves away from the minima ( $\pi/6, 3\pi/6, \dots$ ) shown in Figure 2, we set the integration range of eq 14 from  $+\infty$  to  $-\infty$ . Furthermore, for this pathway we have to modify eq 12 to account for the participation of hindered motion. The sums over  $j'jm'$  as well as  $Q_{rot}(T)$  in eq 12 have to be replaced by the corresponding sum over the librational motion, which is  $Q_{lib}^{-1} \sum_{\nu_h, \nu_h'} e^{-(\nu_h + 1/2)\hbar\omega_{lib}/kT}$  for  $\nu_h \rightarrow \nu_h'$  and the two-state partition function  $Q_{lib} = (1 + e^{-\hbar\omega_{lib}/kT}) e^{-1/2\hbar\omega_{lib}/kT}$ . At 85 K, the contribution of the  $0 \rightarrow 0$  (hindered-to-hindered) transition to the overall deexcitation probability given by eq 12 is  $3.13 \times 10^{-10}$ . The contribution is  $9.25 \times 10^{-11}$  at 50 K and decreases to a value as low as  $1.57 \times 10^{-12}$  at 10 K. For  $0 \rightarrow 1$ , the corresponding three values are  $7.71 \times 10^{-12}$ ,  $2.28 \times 10^{-12}$ , and  $3.88 \times 10^{-14}$ , respectively. Note that for  $0 \rightarrow 0$ , as well as  $1 \rightarrow 1$ ,  $(E_{\nu_h'} - E_{\nu_h}) = 0$ , so the entire vibrational energy is transferred to local translation and phonon modes,  $\Delta E_{k'k} = \hbar\omega - (E_{k'} - E_k)$ .

Next, we now consider transitions among high-lying free rotational states ( $j > 8$ ) with  $jm = j'm'$ , where the amount of energy transferred to local translation is  $\Delta E_{k'k}$  and to the host phonon modes is  $(E_{k'} - E_k)$  as in  $\nu_h \rightarrow \nu_h'$  transitions discussed above. In determining  $P_{01}(T)$ , we sum  $P_{0j'm'k,1jmk}(T)$  over  $m'$  (e.g., for  $j' = 6$ ,  $m' = 0, \pm 1, \dots, \pm 6$ ), and average over  $2j + 1$   $m$  values. At 50 K, for example, the contribution of  $j = j' = 9$ , the lowest free rotational state, to  $P_{01}(T)$  is  $9.62 \times 10^{-13}$ , whereas the contribution from  $j = j' = 11$  is only  $2.81 \times 10^{-13}$ .

When  $j' > j$ , the rotational motion takes part of the vibrational energy intramolecularly, thus causing a smaller amount of energy transfer to local translation and phonon modes than the  $jm = j'm'$  case. The first of such free-to-free rotational transitions is  $jm = 90 \rightarrow j'm' = 100$ , but its probability is negligible. At 85 K, the contribution from this  $\Delta j = 1$ ,  $\Delta m = 0$  case is only  $1.63 \times 10^{-18}$ . However, for  $90 \rightarrow 110$ , the probability is  $6.26 \times 10^{-12}$ , which is about one-seventh of the leading contribution coming from  $90 \rightarrow 90$ , a  $\Delta j = 0$ ,  $\Delta m = 0$  case. A similar picture emerges for the cases with  $j = j'$ , but  $m \neq m'$ . These results indicate that the differences in probabilities are consistent with the predictions of the selection rules of  $\Delta j = 0, \pm 2$  and  $\Delta m = 0, \pm 2$ .

It is important to note that the selection rules hold for the ideal interaction system with simple angle dependence. In the present model, the angle between the molecular axis and the center of cage-to-argon 1 axis is  $\theta$ , but the corresponding angles for all other Ar atoms are different from  $\theta$ . If the latter interactions were absent (i.e., a simple atom-diatom collision) and if the perturbation energy was obtained by expanding the atom-atom distances between argon 1 and  $O_2^-$  for small values of  $x/l$ , we would find the angle dependence of the leading term to be  $\cos^2 \theta$ , for which the selections rules of free-to-free rotational transitions are precisely  $\Delta j = 0, \pm 2$  and  $\Delta m = 0, \pm 2$ . In the present interaction system consisting of 12 host atoms, we can view many-body interactions in the cage as a sequential event. Consider that one of the oxygen atoms, e.g.,  $O_A$ , is the closest to argon 1 at one instant, and it then moves to close proximity of another atom, e.g., argon 7, at the next instant as  $O_2^-$  rotates. At the first instance, the  $O_A$ -argon 1 interaction is the main event, but as  $O_2^-$  rotates, the  $O_A$ -argon 7 interaction becomes the main event, and so on. A similar sequence occurs at the other side for  $O_B$ . The  $\theta$  dependence seen in Figure 2 is the manifestation of such periodic behavior. Even though the  $\theta, \phi$  dependence of  $U(L_n, x, \theta, \phi)$  given by eq 3 appears complicated, this behavior is embedded in the potential function, eventually leading to the selection rules that approximately follow the ideal relations mentioned above. The transition probabilities of  $jm \rightarrow j'm'$ , including  $jm = j'm'$ , displayed above support this statement; for example,  $4.21 \times 10^{-11}$ ,  $1.63 \times 10^{-18}$ , and  $6.26 \times 10^{-12}$  for  $90 \rightarrow 90$ ,  $90 \rightarrow 100$ , and  $90 \rightarrow 110$ , respectively. The probabilities of intermultiplet transitions are significantly smaller than those of  $\Delta m = 0$ . Furthermore, for a given set of  $jj'$ , all contributions have to be summed over  $m$  and then averaged over  $m'$ , so the combined contribution of the  $jm$  set is much smaller than the leading term  $j0 \rightarrow j0$ .

Still another energy transfer pathway is the hindered-to-free type for which the initial state in eq 13 is  $|0\rangle$ . In this case, the  $jm$ -sum and  $Q_{\text{rot}}(T)$  have to be replaced by  $Q_{\text{lib}}^{-1} \sum_k e^{-(\nu_h + 1/2)\hbar\omega_{\text{lib}}/kT}$  and  $Q_{\text{lib}} = (1 + e^{-\hbar\omega_{\text{lib}}/kT})e^{-1/2\hbar\omega_{\text{lib}}/kT}$  in eq 12 as in the hindered-to-hindered case, but retaining the  $j'm'$ -sum for the final state of the free rotation case. The most important transition among this type is  $\nu_h = 0 \rightarrow j'm' = 90$ , for which the probability is  $1.04 \times 10^{-12}$  at 85 K. At 50 K, the probability decreases to  $3.08 \times 10^{-13}$  and is as small as  $5.25 \times 10^{-15}$  at 10 K. For  $0 \rightarrow 91$ , the probability is only  $2.52 \times 10^{-15}$  at 85 K but increases to  $4.17 \times 10^{-13}$  for  $0 \rightarrow 92$ . Although no specific selection rules apply to these transitions, we note that the probability for even  $m'$  is much larger than that for odd  $m'$ .

Our results reported above indicate the most important energy transfer pathway is the  $0 \rightarrow 0$  and  $1 \rightarrow 1$  hindered-to-hindered transition, in which the vibrational energy of  $O_2^- (\nu=1)$  transfers to the local translational and phonon modes. The contribution

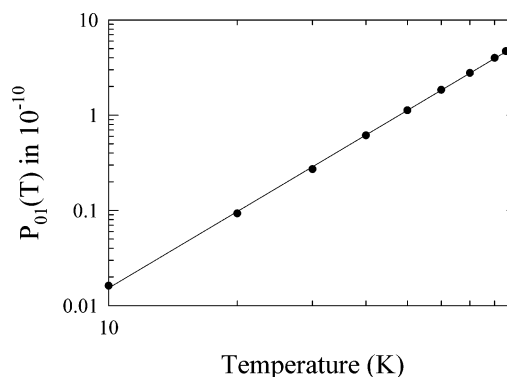


**Figure 3.** Temperature dependence of the energy transfer probability  $P_{01}(T)$  on a log-log scale.

of  $0 \rightarrow 1$ , in which part of the vibrational energy deposits in the hindered motion, is far less important compared to those of the  $0 \rightarrow 0$  and  $1 \rightarrow 1$  transitions. These two transitions are followed by free-to-free transitions, in particular the transitions of the type  $jm = j'm'$ , in which the energy is also transferred to local translation and phonon modes. The relaxation process also involves  $jm \neq j'm'$  rotational transitions, but the contribution of such free-to-free transitions to the overall relaxation process is not important. The least efficient pathway is hindered-to-free transitions, in which the vibrational energy is transferred to rotation intramolecularly via multiquantum transitions, in addition to energy transfer to local translation and argon modes. The sum of all these contributions is the overall energy transfer probability  $P_{01}(T)$  defined by eq 12. The energy transfer probability is  $4.70 \times 10^{-10}$  at 85 K and decreases to  $1.12 \times 10^{-10}$ , when the temperature is lowered to 50 K. At 10 K, it is as small as  $1.62 \times 10^{-12}$ . These results indicate that the energy transfer probability varies 2 orders of magnitude over the condensed-phase temperature range considered in the study. As shown in Figure 3, the temperature dependence can best fit to the linear relation in a log-log plot. This temperature dependence is radically different from the well-known linear relation  $\log P_{01}(T) \propto T^{-1/3}$ , originally formulated by Landau and Teller for vibrational relaxation in the gas phase.<sup>33</sup>

**B. Relaxation Rate Constants.** An important quantity needed in studying energy transfer processes is the vibrational relaxation rate constant  $k$ , which can be calculated by combining  $P_{01}(T)$  with a collision frequency. Unlike in gas-phase collisions, collision frequencies in the condensed phase are difficult to estimate because the concept of a collision in the phase is less well-known, especially for the guest trapped in a solid matrix. In the condensed phase, it is unclear what constitutes an individual collision as it is difficult to determine when the first collision ends and the second begins in the environment of many host atoms. Even if the occurrence of individual collisions is established, it is not trivial to establish how such collisions affect the outcome of the overall energy relaxation process. It is simple to visualize in Figure 1a the situation that when the guest collides with, e.g., argon 1, its interaction with nearby host atoms, i.e., atoms 2, 6, 7, and 10, is also important. The interaction of a guest molecule with its host atoms is continuous, because each guest-host collision is part of the overall encounter, leading to vibrational relaxation in the condensed phase. In the cage environment, what is important in determining the relaxation process is not a well-defined single collision event but the encounter that encompasses a series of collisions. As noted in section IV, the c.m. of  $O_2^-$  undergoes a one-half period oscillation around the cage center, and one of the two oxygen atoms interacts with the host atoms in one hemisphere, whereas

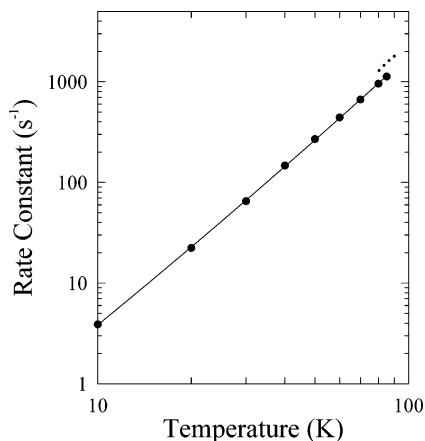


**Figure 4.** Temperature dependence of the relaxation rate constant  $k$  on a log–log scale. The dotted curve is for  $k$  calculated with the cell-model collision frequency in the liquid argon temperature range.

the other interacts with those in the other hemisphere. Thus, the integration range of  $-1/4\tau$  to  $1/4\tau$  for the Fourier integral of local translation is the time scale representing the frequency of occurrence of such encounters in the rigid environment. The excited guest transfers its vibrational energy to other modes during this time interval, which is  $1/2\tau = (\pi l)(\mu/2V_0)^{1/2}$ , so the relaxation rate constant can be expressed as

$$k = (1/2\tau)^{-1} P_{01}(T) \quad (15)$$

The numerical value of the frequency of collisions is  $(1/2\tau)^{-1} = 2.40 \times 10^{12} \text{ s}^{-1}$ ; i.e., in the cage environment the guest is in contact with the host atoms suffering perturbation at a rate of  $10^{12}$  times per second. The latter value is comparable to the collision frequencies determined in other models. For example, using the Slater equation for an assembly of quantized, energy-weighted normal modes, Wiesenfeld has calculated the collision frequency of  $3.1 \times 10^{12} \text{ s}^{-1}$  for HCl + Ar at temperatures 9–20 K.<sup>34</sup>

When we use  $(1/2\tau)^{-1}$  for the collision frequency, the contribution of the  $0 \rightarrow 0$  hindered-to-hindered transition to the rate constant at 50 K is as large as  $222 \text{ s}^{-1}$ ; i.e., the energy transfer occurs on a millisecond time scale. The next most efficient pathway is the  $v_h = 1 \rightarrow v_h = 1$  hindered-to-hindered transition, which is  $37.5 \text{ s}^{-1}$ , followed by  $5.46 \text{ s}^{-1}$  for  $0 \rightarrow 1$  and  $2.31 \text{ s}^{-1}$  for the  $j = j' = 9$  free-to-free transition. Note that for the last case, all  $jm$  states are properly summed and averaged over  $m$  and  $m'$  as stated above. For  $j = j' = 10$ , the rate constant is  $1.29 \text{ s}^{-1}$ . It is only  $0.740 \text{ s}^{-1}$  for the  $v_h = 0 \rightarrow j' = 9$  transition. At higher temperatures, the contribution of free-to-free rotational transitions tends to become larger than that of the  $0 \rightarrow 1$  hindered-to-hindered transition. The values of the overall rate constant  $k$ , which include all these contributions, are presented by a log–log plot in Figure 4 over the temperature range of 10–85 K. At 70 and 85 K, the values of  $k$  are 665 and  $1130 \text{ s}^{-1}$ , respectively. The rate constant is  $270 \text{ s}^{-1}$  at 50 K and decreases to a much smaller value of  $3.88 \text{ s}^{-1}$  at 10 K. The plot shown in Figure 4 closely follows the linear relation  $k \propto T^c$ , i.e.,  $\log k \propto \log T$ , where  $c = 2.7$  is an exponent characteristic of the present condensed-phase relaxation process taking place at and near cryogenic temperatures.

The collision frequency in liquids can be determined in a cell model as  $z = (8kT/\pi\mu)^{1/2}/(2^{1/2}\rho^{-1/3} - \sigma_c)$ ,<sup>35–37</sup> where  $\rho$  is the number density and  $\sigma_c$  is the collision diameter. Extrapolating linearly the experimental densities 22.15 and  $22.64 \text{ nm}^{-3}$  at the mole fractions  $X_{\text{O}_2} = 0.3$  and 1.0 for  $\text{O}_2 + \text{Ar}$  to  $X_{\text{O}_2} =$

0, we find  $21.95 \text{ nm}^{-3}$ .<sup>19,38,39</sup> Note that these density data are obtained at 77 K, but the extrapolated values change only slightly in the temperature range considered in the present study. At 85 K,  $z$  is found to be  $3.29 \times 10^{12} \text{ s}^{-1}$ , which is about 40% larger than the value of  $(1/2\tau)^{-1}$  given above. At the solid argon temperature of 50 K, it is  $3.52 \times 10^{12} \text{ s}^{-1}$ , which are comparable to the value of  $(1/2\tau)^{-1}$ . In Figure 4, we have extended the solid curve obtained for the rigid environment to this narrow liquid temperature range, e.g.,  $(1/2\tau)^{-1}P_{01}(T) = 1130 \text{ s}^{-1}$  versus  $zP_{01}(T) = 1540 \text{ s}^{-1}$  at 85 K. The dotted curve at the upper end of the temperature range is obtained by using the cell model expression, but its difference from the result of eq 15 is not large. Note that if we apply the cell model expression near the low end temperature end considered in Figure 4, the resulting rate constant is significantly smaller than that obtained from eq 15. For example, at 10 K, we obtain  $1.83 \text{ s}^{-1}$ , which is smaller than the result of eq 15 by a factor of 2.

Our results presented in Figure 4 indicate that vibrational relaxation time scales for  $\text{O}_2^-(\nu=1)$  in an argon cage range from millisecond to second in the temperature range. These values are 2 orders of magnitude larger than the experimental and calculated values of  $\text{O}_2(\nu=1) + \text{Ar}$ , but they still represent a very slow relaxation process for the molecular ion in an argon cage. For  $\text{O}_2 + \text{Ar}$ , the rate constant is known to be  $23 \text{ s}^{-1}$  at 85 K and  $5.1 \text{ s}^{-1}$  at 50 K; it is as low as  $0.015 \text{ s}^{-1}$  at 10 K.<sup>3</sup> Extrapolating their observed data for neat liquid  $\text{O}_2$  and high mole fraction mixtures ( $\text{O}_2 + \text{Ar}$ ), Faltermeier, Protz, Maier, and Werner estimated the optimum value of  $k$  in the limit  $X_{\text{O}_2} \rightarrow 0$  as  $12 \text{ s}^{-1}$  at 77 K.<sup>17</sup> The rate constant estimated by Everitt and Skinner at 85.5 K is  $25 \text{ s}^{-1}$ .<sup>19</sup> For the near-homonuclear molecule CO in Ar at 8–24 K, the rate constant is known to be less than  $10 \text{ s}^{-1}$ .<sup>40</sup> For  $\text{C}_2^-(X^2\Sigma_g^+)$  in Ar at the cryogenic temperature range of 14–30 K, the measured  $k$  is known to be  $\sim 6.8 \text{ s}^{-1}$ .<sup>41</sup> The rate constant of the present calculation varies from  $3.90 \text{ s}^{-1}$  at 10 K to  $65.1 \text{ s}^{-1}$  at 30 K. The fundamental frequency of  $\text{C}_2^-$  is  $1781 \text{ cm}^{-1}$ ,<sup>26</sup> which is significantly larger than that of the present system ( $1090 \text{ cm}^{-1}$ ), so a larger amount of vibrational energy has to be removed from the excited molecular ion; i.e., the relaxation is slower in  $\text{C}_2^-$  compared  $\text{O}_2^-$ . However, the decrease is modest in the present model, where the trajectory of local translation is a sinusoidal function, giving the Fourier integral less strongly dependent on the frequency compared to other models, such as the hyperbolic trajectory of gas-phase collisions.<sup>42</sup> In addition to the frequency difference, we note that the bond distance of  $\text{C}_2^-$  is  $1.268 \text{ \AA}$ , which is somewhat shorter than that of the present system ( $1.35 \text{ \AA}$ ). A smaller molecular ion can undergo less hindered motion in the cage, in which case free-to-free rotational energy transfer becomes a significant energy transfer step but the step is less efficient in removing the vibrational energy than the transitions involving hindered motions. Therefore, the differences in vibrational frequencies and bond distances that lead to the relaxation rate of the  $\text{C}_2^- + \text{Ar}$  system in a cryogenic environment are much smaller than those for  $\text{O}_2^- + \text{Ar}$ , even though both systems have the important contribution of the induction energy.

To emphasize the importance of the induction energy in the vibrational relaxation of molecular ions, we note that the depth of the attractive potential of the LJ interaction of Ar to  $\text{O}_2$  is  $0.0102 \text{ eV}$  occurring at the equilibrium separation of  $3.92 \text{ \AA}$ . On the other hand, when the induction energy is included for  $\text{O}_2^- + \text{Ar}$ , the well depth becomes as deep as  $0.0801 \text{ eV}$  occurring at  $3.40 \text{ \AA}$ . Thus, for  $\text{O}_2^-$  interacting with 12 Ar atoms, the contribution of the induction energy to the overall interaction

potential can be particularly important. The induction energy has two important effects on the vibrational relaxation: (a) it “speeds” up the translational motion of  $O_2^-$  toward Ar so that the kinetic energy of the relative motion is increased, and (b) it increases the slope of the repulsive wall of the interaction potential on which the probability of energy transfer depends sensitively. These effects lead to the molecular ion reaching a deeper repulsive region, where the slope of the potential wall rises sharply, for a greater perturbation of the interaction modes, which participate in the vibrational relaxation of  $O_2^-$ , thus enhancing the relaxation process in the cage over that of the unchanged guest molecule.

Finally, we note that in the above calculation, we have only considered one-phonon processes for the participation of host atoms in the relaxation process. The effects of multiphonon processes can be considered similarly. For two-phonon processes, for example, the major difference from the above treatment is that eq 5 will then contain the second derivative of  $U(L_{n,x}, \theta, \phi)$  with respect to  $q_n$  and the coordinates  $\delta^2 q_n^2 x$  with  $s = 5$ . Thus, the perturbation energy is different from the single-phonon case, but the main difference appears in the matrix element of  $q_n^2$  and the Fourier integral that contains the inelasticity term  $\Delta E_{j,j',k,k'}$ , which now represents a larger amount of energy transferring to the host atoms with  $k' = k + 2$ . The ratio of the matrix element of two-phonon transitions to that of single-phonon transitions is

$$\Gamma^{-2} (\hbar/2M_{Ar}\omega_{Ar}) \sum_k^{\infty} (k+1)(k+2) \times \exp(-k\hbar\omega/kT) \sum_k^{\infty} (k+1) \exp(-k\hbar\omega/kT)$$

which takes the values of 0.0281, 0.0178, and 0.00619 at 85, 50, and 10 K. The square of the Fourier integral in eq 9 for the two-phonon process is smaller than that for the one-phonon case by a factor of 3.12. Thus the combination of these two factors leads to the two-phonon process smaller than the one-phonon case by  $9.00 \times 10^{-3}$ ,  $5.70 \times 10^{-3}$ , and  $1.98 \times 10^{-3}$  at 85, 50, and 10 K, respectively. Other factors in the perturbation energy also affect the comparison, but the main difference is determined by these two factors, attesting that contribution from two-phonon process is much smaller than the one-phonon process considered above.

## VI. Concluding Comments

The vibrational relaxation of  $O_2^- (v=1)$  in a cage of one full argon shell is studied in the temperature range 10–85 K using semiclassical procedures. The interaction model is based on the trapped molecular ion undergoing local translation and hindered and free rotation in the cage composed of 12 host atoms. Local translation undergoes a sinusoidal motion around the cage center. Low-lying rotational energy levels are hindered, and high-lying levels are free, thus leading to the participation of hindered-to-hindered, hindered-to-free, and free-to-free rotational transitions in the relaxation process.

The primary energy transfer pathway for the relaxation of  $O_2^-$  is from vibration to local translation accompanied by energy transfer to argon's phonon modes, whereas hindered rotation remains in a librational state. This pathway is followed by energy transfer to free-to-free rotational transitions and hindered-to-

free rotational transitions. The overall de-excitation probability is on the order of  $10^{-12}$ , representing extreme difficulty of the excited molecule relaxing in the cage environment. The rate constant  $k$  of the relaxation process varies from  $1130 \text{ s}^{-1}$  at 85 K to  $3.88 \text{ s}^{-1}$  at 10 K, a decrease by 3 orders of magnitude. Despite the high collision frequency of the order of  $10^{12} \text{ s}^{-1}$ , vibrational energy relaxation time scales for the molecular ion in an argon cage range from milliseconds to seconds. The temperature dependence closely follows the linear relation of  $\log k \propto \log T$ .

## References and Notes

- Jellinek, J.; Beck, T. L.; Berry, R. S. *J. Chem. Phys.* **1986**, *84*, 2783.
- Jakowski, J.; Klos, J.; Chalasinski, G.; Severson, M. W.; Szczesniak, M. M.; Cybulski, S. M. *J. Chem. Phys.* **2000**, *112*, 10895.
- Shin, H. K. *J. Chem. Phys.* **2004**, *121*, 9443.
- Abbate, A. D.; Moore, C. B. *J. Chem. Phys.* **1985**, *82*, 1255.
- Raff, L. M. *J. Chem. Phys.* **1991**, *95*, 8901; **1992**, *97*, 7459.
- Somasi, S.; Khomami, B.; Lovett, R. *J. Chem. Phys.* **2000**, *113*, 4320.
- Ikeshoji, T.; Torchet, G.; de Feraudy, M.-F.; Koga, K. *Phys. Rev. E* **2001**, *63*, 031101.
- Ning, X.-J.; Qin, Q.-Z. *J. Chem. Phys.* **1999**, *110*, 4920.
- Dahoo, P. R.; Lakhliifi, A.; Chabbi, H. *J. Chem. Phys.* **1999**, *111*, 10192.
- Mossa, S.; Tarjus, G. *J. Chem. Phys.* **2003**, *119*, 8069.
- McGaughey, A. J. H.; Kaviani, M. *Phys. Rev. B* **2004**, *69*, 094303.
- Papanikolas, J. M.; Gord, J. R.; Levinger, N. E.; Ray, D.; Vorsa, V.; Lineberger, W. C. *J. Phys. Chem.* **1991**, *95*, 8028.
- Greenblat, B. J.; Zanni, M. T.; Neumark, D. M. *J. Chem. Phys.* **1999**, *111*, 10566.
- Davis, A. V.; Wester, R.; Bragg, A. E.; Neumark, D. M. *J. Chem. Phys.* **2003**, *119*, 2020.
- Shin, H. K. *Adv. Chem. Ser.* **1966**, *58*, 44.
- Yardly, J. T. *Introduction to Molecular Energy Transfer*; Academic: New York, 1980; Chapter 6.
- Faltermeier, B.; Protz, R.; Maier, M.; Werner, E. *Chem. Phys. Lett.* **1980**, *74*, 425.
- Faltermeier, B.; Protz, R.; Maier, M. *Chem. Phys.* **1981**, *62*, 377.
- Everitt, K. F.; Skinner, J. L. *J. Chem. Phys.* **1999**, *110*, 4467.
- Tinti, D. S.; Robinson, G. W. *J. Chem. Phys.* **1968**, *49*, 3229.
- Bondebey, V. E.; Brus, L. E. *J. Chem. Phys.* **1975**, *63*, 794.
- Diestler, D. J.; Knapp, E. W.; Ladouceur, H. D. *J. Chem. Phys.* **1978**, *68*, 4056.
- Shin, H. K. *J. Chem. Phys.* **1981**, *75*, 3821.
- Louisell, W. H. *Quantum Statistical Properties of Radiation*; Wiley: New York, 1973; Chapter 1.
- Karplus, M.; Porter, R. N. *Atoms and Molecules*; Benjamin: New York, 1970; Table 4.2.
- Huber, K. P.; Herzberg, G. *Constants of Diatomic Molecules*; Van Nostrand Reinhold: New York, 1979.
- Hirschfelder, J. O.; Curtiss, C. F.; Bird, R. B. *Molecular Theory of Gases and Liquids*; Wiley: New York, 1967; pp 1110–1111 for  $D$  and  $\sigma$  and p 168 for the combining laws.
- Cambi, R.; Cappelletti, D.; Liuti, G.; Pirani, F. *J. Chem. Phys.* **1991**, *95*, 1852.
- Atkins, P. W.; Friedman, R. S. *Molecular Quantum Mechanics*; Oxford: New York, 1997; Chapter 6.
- Eyring, H.; Walter, J.; Kimball, G. E. *Quantum Chemistry*; Wiley: New York, 1954; pp 358–360.
- Takayanagi, K. *Prog. Theor. Phys.* **1952**, *8*, 497.
- Nikitin, E. E. *Theory of Elementary Atomic and Molecular Processes in Gases*; Oxford: London, 1974; p. 59.
- Landau, L.; Teller, E. *Phys. Z. Sowjetunion* **1936**, *10*, 34.
- Wiesenfeld, J. M. Ph.D. Thesis, University of California, Berkeley, 1977; p 336.
- Litovitz, T. A. *J. Chem. Phys.* **1957**, *26*, 465.
- Madigosky, W. M.; Litovitz, T. A. *J. Chem. Phys.* **1961**, *34*, 489.
- Davis, P. K. *J. Chem. Phys.* **1972**, *57*, 517.
- Johnson, J. K.; Zollweg, J. A.; Gubins, K. E. *Mol. Phys.* **1993**, *78*, 591.
- Sun, T.; Teja, A. S. *J. Phys. Chem.* **1996**, *100*, 17365.
- Dubost, H.; Charneau, R. *Chem. Phys.* **1976**, *12*, 407.
- Allamandola, L. J.; Rohenthal, H. M.; Nibler, J. W.; Chappel, T. *J. Chem. Phys.* **1977**, *67*, 99.
- Shin, H. K. In *Dynamics of Molecular Collisions*; Miller, W. H., Ed.; Plenum: New York, 1976; Part A, p 131.